CCC 2025 **Proceedings of the Creative Construction Conference** (2025)
Edited by: Miroslaw J. Skibniewski & Miklós Hajdu & Žiga Turk
https://doi.org/10.22260/CCC2025/0010

TIME-DEPENDENT CORROSION AND SEISMIC FRAGILITY: A FRAMEWORK FOR LONG-TERM RISK MITIGATION

Gili Lifshitz Sherzer[1], Alon Urlainis[1], and **Igal M. Shohet** [2,3]
[1] *Department of Civil Engineering, Ariel University, Ariel, Israel*
[2] *Department of Civil and Environmental Engineering, Faculty of Engineering Sciences, Ben-Gurion University of the Negev, Beer Sheva, 8410501 Israel*
[3] *Department of Civil and Construction Engineering, Chaoyang University of Technology, 168, Jifeng E. Rd., Wufeng District, Taichung, 41349 Taiwan, R.O.C.*

Abstract

This research introduces a novel procedure for considering corrosion effects within critical infrastructure exposed to seismic risk, focusing on reinforced concrete structures. Most conventionally developed seismic fragility curves cannot assess the progressive material degradation over time, such as corrosion. At the same time, the present study proposes a novel approach that explicitly incorporates corrosion-driven deterioration in seismic vulnerability assessment. The proposed framework couples time-dependent corrosion modelling with FDEM numerical simulations to assess deterioration in structural integrity. These results are used to update seismic fragility curves that accurately capture the increased vulnerability of corroded structures to earthquake-induced damage. The significant contribution of this research is developing an integrated risk assessment model that merges the corrosion-adjusted fragility functions with seismic hazard analysis for long-term seismic risk assessments. The primary novelty within the methodology formulation involves developing a cumulative risk ratio, expressing the overall accumulation of risk during the structure's service life. In this context, this framework has been validated with a case study of a single-story RC moment frame for different corrosion scenarios and spatial distributions. The numerical results agreed well with empirical data by a 3-14% discrepancy for the projected 75-year life cycle period. The results indicate a considerable increase in seismic risk due to corrosion effects: 59% for moderate and 100% for intense corrosion environments. The findings highlight that considering the mechanisms of corrosion during seismic risk assessment allow for more realistic seismic risk assessment and ameliorate critical infrastructures resilience along their service life cycle.

Keywords: Corrosion progression, FDEM, Fragility curves, Reinforced Concrete Structure, Seismic risk analyses.

Peer-review under responsibility of the scientific committee of the Creative Construction Conference 2025.

1. Introduction

Reinforced concrete (RC) structures under corrosive environments experience severe losses in seismic performance when corrosion mechanisms are explicitly modelled [1], [2]. Various research works have demonstrated that the inclusion of time-dependent corrosion effects leads to a notable decrease in structural capacity [3]. For instance, finite element and time-variant modelling approaches report losses of up to 50% in base shear capacity and a rise of 20–25% in the probability of failure within 50 years [3]. Coupled models that reconcile time-dependent corrosion simulation and Finite–Discrete Element Modelling (FDEM) predict even greater risk increases, with moderate corrosion increasing seismic hazard by 59% and intensive corrosion doubling it in 75 years, while case study comparisons find variations of only 3–14% [4]. Notably, FDEM has been successfully validated for simulating fracture and failure in concrete elements [5], supporting its use in corrosion-integrated seismic risk assessments.

Different modelling strategies—from finite difference methods and nonlinear finite element analyses to probabilistic models (often performed using Open Sees or enhanced using neural networks) — have been used to model chloride-induced deterioration, flexural strength loss, ductility loss, and progressive

Corresponding author email address: gili.lifshitz@gmail.com

accumulation of seismic risk over a structure's service life [6]. Other studies have also modelled concrete degradation due to brine attack, highlighting the diverse mechanisms contributing to long-term structural deterioration [7]. All these studies highlight the need for seismic fragility curve updating with cumulative risk ratios and corrosion-incorporated seismic models for more accurate quantification of the increasing vulnerability of deteriorating RC structures under seismic loading.

The diversity of integration methods reflects the inherent difficulty of coupling corrosion development with seismic hazard assessment [6]. The dominance of nonlinear finite element methods and advanced computational frameworks indicates a clear trend toward increasingly sophisticated modelling methods [3]. However, the fact that nearly half of the present work considered herein lacks experimentally or case study validation suggests a very large gap that must be addressed in subsequent endeavours [3], [6], [8]–[11].

The focused interest in time-dependent mechanisms of corrosion and degradation impact is precisely within the research objective of evaluating how deteriorating material degradation influences seismic performance [3]. Additionally, the use of probabilistic models in different studies demonstrates consideration of and compensation for significant uncertainty regarding long-term structural performance for extreme events [12]–[14].

While a few models demonstrate reasonable agreement with experimental measurements or field observations, the overall variety of validation methodologies—and the absence of validation in most cases—indicates the critical need for more rigorous, systematic validation methods [1]. Better validation practices will increase corrosion-integrated seismic risk models' credibility and applicability to infrastructure resilience planning.

The significance of this research is the improvement of the precision and validity of long-term seismic risk evaluation for critical infrastructure. By explicitly accounting for corrosion effects, the study offers a more realistic estimation of structure vulnerability, thus facilitating improved maintenance planning, resource allocation, and risk mitigation measures. This enhancement is crucial in enhancing essential infrastructure resilience and operational reliability in seismically active and corrosive environments.

2. Methodology

The research proposes a time-dependent corrosion-integrated risk assessment system for reinforced concrete wall subjected to seismic actions. There are four main steps in the methodology (see Fig. 1):

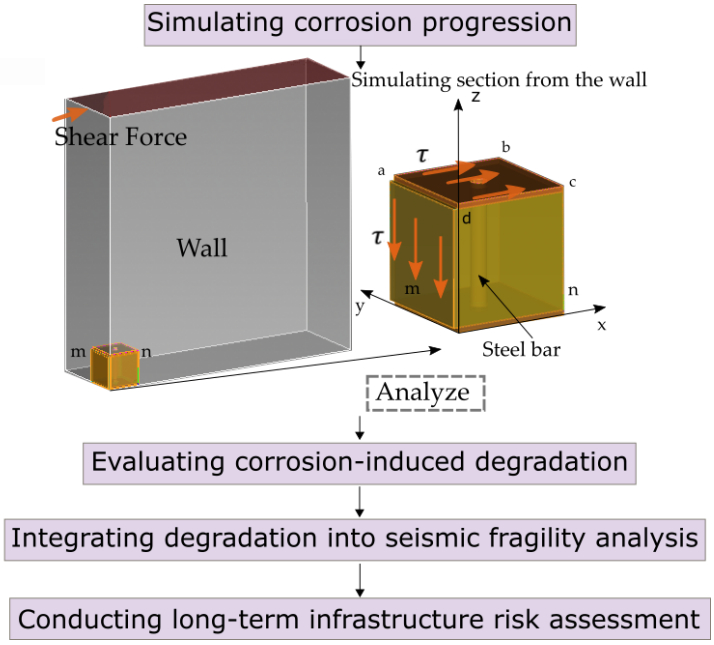

Fig. 1. Methodology flowchart.

The evolution of damage and its effect on structural capacity are simulated and presented in this section. Exposure levels of corrosion are defined following Raoul François [15], based on which current densities equal to 0.2, 1.0, and 3.5 μA/cm² are assumed to model minor, moderate, and intensive corrosion, respectively.

- Simulation takes place for a period of 120 years, replicating the evolution from the passive to severe corrosion states. For each time increment:
- Internal pressure and shear boundary conditions are applied to a concrete cube model extracted from the wall to model local effects.
- Automated simulations assess the progressive degradation in structural response and shear capacity due to seismic loading.

3. Framework Development

3.1. Mechanical Model

Simulations were carried out on a 116 × 116 × 116 mm³ concrete block removed from the base of a wall — where seismic shear forces are most significant, to save computation time. Reinforcement rigidity was omitted, but circumferential pressure due to corrosion was imposed as an internal boundary condition over a meshed cylindrical hole for the rust extension effect.

Seismic loading was simulated with incremental shear stress up to failure, where the back of the cube faces confinement and free boundaries at all other locations. Internal pressure and material degradation were updated after de-passivation, assumed to occur after 20 years, based on corrosion initiation findings reported in [16], [17]. Empirical equations (Eqs. 1–9) were assigned to the material to simulate degradation mechanical properties like compressive strength, tensile strength, modulus of elasticity, and cohesion due to corrosion products. The degradation of concrete properties was driven by corrosion expansion, which influences crack width and reduces shear capacity (Eq. (1)).

$$f_{ck}^{*} = \frac{f_{ck}}{1+k_r\frac{\varepsilon_1}{\varepsilon_{co}}}, \tag{1}$$

where k_r is taken as 0.1 for medium-diameter ribbed bars for allowing roughness and bar size [18], and ε_{co} (0.002) is the peak compressive strain according to IS 456 [19]. ε_1 captures the tensile strain associated with cracking subjected to compression, as defined in Eq. (2).

$$\varepsilon_1 = \frac{b_f - b_o}{b_0}, \tag{2}$$

b_0 is the original cross-sectional width without corrosion cracks, while b_f represents the expanded width due to corrosion-induced cracking. The increase in thickness is estimated using Eq. (3).

$$b_f - b_o = n_{bars} w_c, \tag{3}$$

where n_{bars} represents the number of bars in each layer, and w_c denotes the crack width corresponding to a given level of corrosion over the time interval Δt, as defined by Eq. (4).

$$w_c = 2\pi(v_{rs} - 1)d_e, \tag{4}$$

where v_{rs} is corrosion product expansion to intact steel volumetric ratio, generally assumed to be 2 [64], and d_e is the corrosion penetration depth, computed from Eq. (5).

$$d_e = 0.0115 i_{co} t, \tag{5}$$

where i_{co} is the corrosion current density (in cm/year), and t is the elapsed time since the corrosion propagation initiation (in years). The concrete elastic modulus (E_c) is related to its compressive strength

(f_{ck}) at all stages of its service life, according to the model proposed by Noguchi and Nemati [65], as given in Eq. (6).

$$E_c = 2.1 \times 10^5 (\frac{\gamma}{2.3})^{1.5} (\frac{f_{ck}}{200})^{0.5}, \quad (6)$$

The strength in compression (f_{ck}) and modulus of elasticity of concrete (E_c) is in kg/cm² units with the concrete density (γ) maintained constant at 2.5 ton/m³. Direct tensile strength (f_t) may be approximated from reliable values under conditions where size is not a problem. According to ACI 318 [20] and ref. [21], [22], (f_t) is expressed in relation to (f_{ck}) as follows following Eq. (7), and the model is refreshed at each time step by the following equation:

$$f_t = 0.33\lambda\sqrt{f_{ck}} \ (MPa\ units) \quad (7)$$

Where λ is for lightweight concrete, and in this research, it is taken to be 1.0.

The strength of cohesion (c) and the normal stress (σ_n) in FDEM are incorporated depending on the method as described in [23]:

$$f_s = c + \sigma_n tan\ (\theta_i) \quad (8)$$

where θ_i denotes the friction angle and fs the intrinsic shear strength, the shear strength is approximately proportional to the compressive strength to the 1/2–1/3 power [24].

$$f_s = \sqrt{f_{ck}} \quad (9)$$

The internal pressure P is derived from steel expansion and concrete confinement, as expressed in equations (Eqns. 10–18).

Several models have been proposed for rusting prediction. Andrade et al. (1993) [25] formulated a linear model based on Faraday's law, relating corrosion current density (i_{corr} in μA/cm²) to a reduction in steel bar diameter, using a conversion factor 0.023 (μA/cm² to mm/year).

$$D_{rb} = D_b - 0.023 i_{corr} \Delta t\ (mm) \quad (10)$$

where D_{rb} is the residual steel diameter, D_b is the original diameter, and Δt is the time elapsed since corrosion started.

$$\Delta V_s = \frac{0.023}{2} \times \pi D_b i_{corr} \Delta t\ (mm^3/mm) \quad (11)$$

Assuming uniform corrosion, the radius reduces from R_b, as per Eq. (12), based on the volume loss of steel per unit length, detailed in Eq. (11)

$$R_{rb} = \sqrt{(R_b^2 - {\Delta V_s}/{\pi}}\ (mm) \quad (13)$$

The steel radius accounting for the rust layer is defined as follows:

$$R_r = R_{rb} + \delta o (mm) \quad (14)$$

The total volume of oxide produced is given by: $\Delta V_r = \Delta V_s \rho_s / (\rho_r r_m)$, is the proportion of iron molecular weight to rust molecular weight, as 0.622. To account for the effect of corrosion product migration into open cracks (see figure 5 (e)), we used a modified equation presented in [26]. The modification involves subtracting the volume of available crack space vac into which the oxide penetrates—from the total oxide volume generated by corrosion ΔV_r:

$$\Delta V = \Delta V_r - V_{ac} (mm^3/mm) \quad (15)$$

In addition, we followed the work of [26], which also reduced the thickness of porous layer t_f, and calculated the oxide thickness δ_o as follow:

$$\delta_0 = \sqrt{(R_{rb}^2 + {\Delta V_r}/{\pi}} - R_{rb} - t_f(mm) \quad (16)$$

By applying an equivalent pressure around the steel, the expansion of the corroding reinforcement is simulated. The first step in this process is to calculate effective, non-dimensional mass loss:

$$\gamma = \frac{\frac{(D_b+\delta o\times 2)^2}{D_b^2}-1}{\beta-1} \quad (17)$$

Where β denotes the density of steel divided by density of rust. The strain resulting from the unrestrained expansion of the reinforcement can be determined as follows:

$$E_{s,eq} = \frac{1+\gamma(\beta-1)}{\frac{1-\gamma}{E_S}+\frac{\gamma\beta}{E_O}}\ (GPa) \quad (18)$$

where Es denotes the modulus of elasticity of steel (200 GPa), and E0 refers to the modulus of the elasticity of the oxide in this work taken as (7 GPa).

The internal pressure (P) denotes the confinement effect of the concrete on steel, dependent on the degree of corrosion, calculated in Eq. 19:

$$P = E_{s,eq} \times \varepsilon_{s,free}\ (MPa) \quad (19)$$

3.2. Degradation Analysis and Shear Capacity Loss

Simulated cubes were loaded until failure at each time step, capturing surface crack development and failure modes. Simulated cubes were loaded to failure at each time step, including surface crack growth and failure modes. Shear capacity was verified from each model's shear stress–displacement curves. The capacity at times t_i to t_{i+1} were normalized to the initial capacity at t=0 to evaluate the deterioration as a function of time, shown in Fig. 2.

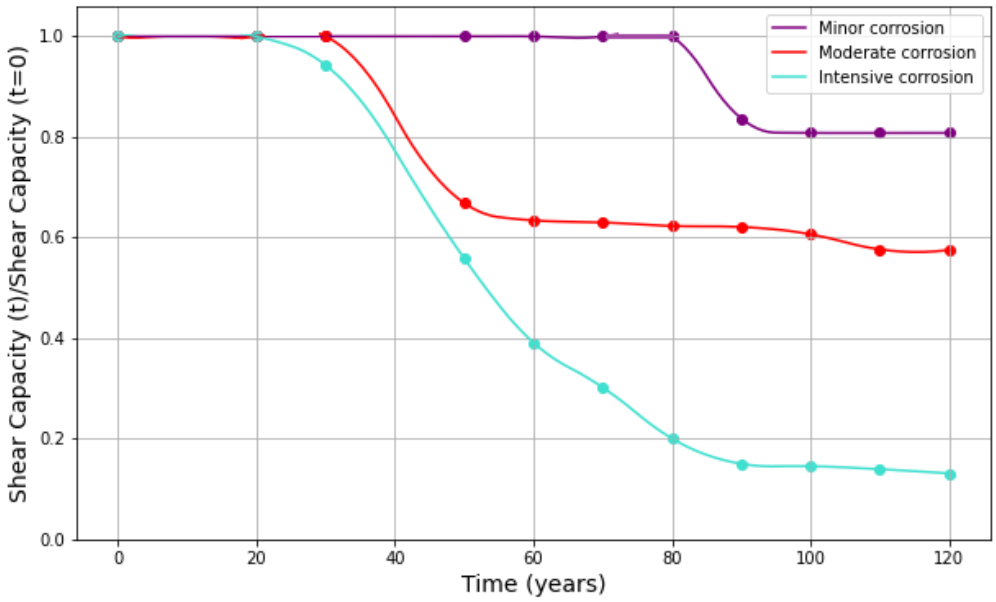

Fig. 2. Shear capacity degradation over time under varying corrosion intensities.

Fig. 1 illustrates progressive shear capacity loss with time for a seismically loaded wall under three corrosion intensities: minor, moderate, and intensive. The results show a trend of capacity reduction of between 20% and greater than 80% after 120 years, based on the intensity of corrosion.

The model focused on a small portion of wall to get detail as against high cost, so the effects of localized corrosion and the shear degradation could be assessed. Though the direct steel contribution to the structural stiffness was neglected, the pressure due to corrosion in the surrounding concrete was considered.

Simulations were done discontinuously, incrementally applying shear load at each time step and modelling material degradation through empirical relationships. While the simplifications, the model adequately captures the trend of degradation, allowing for long-term planning of maintenance and highlighting the importance of early intervention to ensure structural resilience.

3.3. Integrating Corrosion Effects into Seismic Fragility Curves

Reinforced concrete (RC) deterioration is included in the seismic vulnerability analysis for this section based on capacity reduction evaluated previously.

Seismic vulnerability is evaluated using seismic fragility curves, which express the probability of reaching a damaged state (DS) as a function of an earthquake intensity measure (IM). The fragility function is lognormal cumulative distributed [27], [28] and has two parameters: the median structural capacity θ_{ds} and the logarithmic standard deviation β_{ds}, defined as Eq. (19):

$$P\left[DS \geq ds|IM = x\right] = \Phi\left(\frac{ln(x/\theta_{ds})}{\beta_{ds}}\right) ; ds \in \{1,2, \dots N_{DS}\} \tag{20}$$

Where P is the probability of reaching or exceeding a damage state, DS is the damage state index, IM is the intensity measure (e.g., PGA, PGD, PGV), Φ is standard normal cumulative distribution function,

For more than one damage state in order of increasing severity, the probability of being in a certain state is given as:

$$P(DS = ds_i|IM) = \begin{cases} 1 - P(DS \geq ds_i|IM) & i = 0 \\ P(DS \geq ds_i|IM) - P(DS \geq ds_{i+1}|IM) & 1 \leq i \leq n-1 \\ P(DS \geq ds_i|IM) & i = n \end{cases} \tag{21}$$

Baseline Fragility Curves: represent the initial seismic vulnerability of the structure before considering corrosion, founded on parameters available from literature and existing databases [29], [30].

Adjusted Fragility Curves: To incorporate corrosion effects, the median capacity is adjusted using a degradation factor (t), which is calculated as a function of corrosion level (CL) and elapsed time (t). The adjusted median capacity (t) is calculated as:

$$\theta'_{ds_i}(t) = \theta_{ds_i} \cdot f_{CL}(t) \tag{22}$$

Where θ (t) is adjusted median capacity at time, f_{CL} (t) is degradation factor, reflecting corrosion severity over time, CL is corrosion level (minor, moderate, intensive).

To validate the degradation rates, a comparison was done with the findings of Cui et al. [31], which investigated fragility deterioration for RC bridges in marine environments for 0, 25, 50, 75, and 100 years.

The comparison resulted in a close match within 3–14% for the first 75 years, to the advantage of the reliability of the approach. At 100 years, our models resulted in moderately more conservative predictions.

4. Future research and limitations of the present research

While this study offers valuable information, several limitations must be acknowledged. The accuracy of the result depends significantly on the reliability of input data, particularly corrosion rates and structural

characteristics. Future research may possibly greatly improve the modelling framework by enhancing several important areas.

First, reinforcement bar stiffness and the explicit representation of the rebar–concrete interface would increase the accuracy of shear capacity predictions. The discrete degradation model is simulated and gradually loaded by shear stress to failure, whereas degraded mechanical parameters are revised manually according to empirical functions. Crack growth and crack starting should be facilitated with continuous exchange of information from one time step to another, where cracks growing and developing grow progressively, contrary to employing degradation curves.

In addition, bond strength degradation between steel and concrete needs to be simulated because corrosion progressively weakens this interface, which affects load transfer and increases the risk of localized failures, especially under seismic loads. Bond deterioration consideration would provide a more realistic structural deterioration patterns prediction over time.

Further developments should also consider strain rate effects, corrosion-induced voids, and mesoscale deterioration patterns upscaling to the structure level. Finally, input parameter calibration using more detailed field observations and actual-world data acquisition would significantly enhance the model's reliability.

The solution to these points will give a good chance to enhance the proposed methodology and conduct a more accurate long-term corrosion-induced seismic vulnerability assessment in reinforced concrete structures.

5. Conclusions

In this research, a novel strategy towards seismic hazard assessment in reinforced concrete structures of the critical infrastructure considers explicitly the progressive corrosion effects. Results show that seismic load vulnerability grows exponentially in time, markedly for moderate and severe corrosion levels, with cumulative risk ratios rising to six times the baseline over a 120-year lifespan, depending on environmental conditions. One of the important contributions of this study is the development of a corrosion-adjusted fragility method, which allows real-time updates of seismic vulnerability in accordance with corrosion progression. The dynamic assessment reflects more realistic assessments of evolving structural risks, allowing for full lifecycle resilience planning. The case study illustrates the way in which corrosion-adjusted fragility curves signal risk escalation in different geographical and environmental settings.

The findings underscore the significance of factoring time-dependent degradation into seismic risk appraisal, necessitating intensified monitoring, precocious interventions, and active management of infrastructure.

Finally, the current work provides a comprehensive evaluation of seismic resilience in substations according to critical component performance and failure probability. The quantitative indicators and derived fragility curves provide valuable information on post-earthquake operation. The models can be enhanced by introducing more complexity and verified using experimental data from actual events in the future to improve practical applicability.

Acknowledgements

We acknowledge the Ariel HPC Centre at Ariel University for providing computing re-sources that contribute to the research results reported in this paper. Special thanks are extended to Dr. Amit Kashi and Dr. Amir M. Michaelis for their consistent support and expertise in HPC and its applications.

References

[1] E. Afsar Dizaj, R. Madandoust, and M. M. Kashani, “Exploring the impact of chloride-induced corrosion on seismic damage limit states and residual capacity of reinforced concrete structures,” *Struct. Infrastruct. Eng.*, vol. 14, no. 6, 2018, doi: 10.1080/15732479.2017.1359631.

[2] M. Maidi, G. Lifshitz Sherzer, I. Shufrin, and E. Gal, “Seismic Resilience of CRC-vs. RC-Reinforced Buildings: A Long-Term Evaluation,” *Appl. Sci.*, vol. 14, no. 23, p. 11079, 2024.

[3] F. Biondini, E. Camnasio, and A. Palermo, “Lifetime seismic performance of concrete bridges exposed to corrosion,” *Struct. Infrastruct. Eng.*, vol. 10, no. 7, 2014, doi: 10.1080/15732479.2012.761248.

[4] A. Urlainis, G. Lifshitz Sherzer, and I. M. Shohet, “Multi-Scale Integrated Corrosion-Adjusted Seismic Fragility Framework for Critical Infrastructure Resilience,” *Appl. Sci.*, vol. 14, no. 19, p. 8789, 2024.

[5] G. L. Sherzer, Y. F. Alghalandis, K. Peterson, and S. Shah, “Comparative study of scale effect in concrete fracturing via Lattice Discrete Particle and Finite Discrete Element Models,” *Eng. Fail. Anal.*, vol. 135, p. 106062, 2022, doi: https://doi.org/10.1016/j.engfailanal.2022.106062.

[6] A. Alipour, B. Shafei, and M. Shinozuka, “Performance Evaluation of Deteriorating Highway Bridges Located in High Seismic Areas,” *J. Bridg. Eng.*, vol. 16, no. 5, 2011, doi: 10.1061/(asce)be.1943-5592.0000197.

[7] G. L. Sherzer, G. Ye, E. Schlangen, and K. Kovler, “The role of porosity on degradation of concrete under severe internal and external brine attack in confined conditions,” *Constr. Build. Mater.*, vol. 341, no. April, p. 127721, 2022, doi: 10.1016/j.conbuildmat.2022.127721.

[8] L. D. I. Sarno and F. Pugliese, “Critical review of models for the assessment of the degradation of reinforced concrete structures exposed to corrosion,” *SECED 2019 Conf. Earthq. risk Eng. Towar. a resilient world*, no. September, 2019.

[9] F. Cui *et al.*, “Improved time-dependent seismic fragility estimates for deteriorating RC bridge substructures exposed to chloride attack,” *Adv. Struct. Eng.*, vol. 24, no. 3, 2021, doi: 10.1177/1369433220956812.

[10] J. Ghosh and P. Sood, “Consideration of time-evolving capacity distributions and improved degradation models for seismic fragility assessment of aging highway bridges,” *Reliab. Eng. Syst. Saf.*, vol. 154, 2016, doi: 10.1016/j.ress.2016.06.001.

[11] F. Pugliese and L. Di Sarno, “Probabilistic structural performance of RC frames with corroded smooth bars subjected to near- and far-field ground motions,” *J. Build. Eng.*, vol. 49, 2022, doi: 10.1016/j.jobe.2022.104008.

[12] A. Urlainis, I. M. Shohet, and R. Levy, “Probabilistic Risk Assessment of Oil and Gas Infrastructures for Seismic Extreme Events,” in *Procedia Engineering*, 2015, vol. 123, doi: 10.1016/j.proeng.2015.10.112.

[13] G. Lifshitz Sherzer, A. Urlainis, S. Moyal, and I. M. Shohet, “Seismic Resilience in Critical Infrastructures: A Power Station Preparedness Case Study,” *under Rev. possible Publ. Appl*, 2024.

[14] A. Urlainis and I. M. Shohet, “Development of Exclusive Seismic Fragility Curves for Critical Infrastructure: An Oil Pumping Station Case Study,” *Buildings*, vol. 12, no. 6, 2022, doi: 10.3390/buildings12060842.

[15] R. François, “A discussion on the order of magnitude of corrosion current density in reinforcements of concrete structures and its link with cross-section loss of reinforcement,” *RILEM Tech. Lett.*, vol. 6, 2021, doi: 10.21809/rilemtechlett.2021.116.

[16] C. Lu, J. Yang, and R. Liu, “Probability model of corrosion-induced cracking time in chloride-contaminated reinforced concrete,” *Int. Conf. Durab. Concr. Struct. ICDCS 2016*, no. 2011, pp. 309–314, 2016, doi: 10.5703/1288284316150.

[17] K. A. T. Vu and M. G. Stewart, “Structural reliability of concrete bridges including improved chloride-induced corrosion models,” *Struct. Saf.*, vol. 22, no. 4, 2000, doi: 10.1016/S0167-4730(00)00018-7.

[18] D. Coronelli and P. Gambarova, “Structural Assessment of Corroded Reinforced Concrete Beams: Modeling Guidelines,” *J. Struct. Eng.*, vol. 130, no. 8, 2004, doi: 10.1061/(asce)0733-9445(2004)130:8(1214).

[19] BIS, “plain and reinforced concrete—code of practice, Bureau of Indian Standards (BIS),” 2000.

[20] 318 ACI Committee, “Building code requirements for structural concrete (ACI 318-08) and commentary,” 2008.

[21] R. Carrasquillo, A. Nilson, and F. Slate, “Properties of high strength concrete subject to short-term loads,” *J. Proc.*, vol. 78, no. 3, 1981, Accessed: Apr. 04, 2021. [Online]. Available: https://sci-hub.st/https://www.concrete.org/publications/internationalconcreteabstractsportal.aspx?m=details&ID=6914.

[22] B. Fekadu Haile, G. Lifshitz Sherzer, K. Peterson, and G. Grasselli, “Progressive highly stressed volume for size effect analysis,” *Constr. Build. Mater.*, vol. 400, 2023, doi: 10.1016/j.conbuildmat.2023.132600.

[23] Geomechanica, “Irazu 3D Geomechanical Simulation Software. Tutorial Manual,” 2019.

[24] H. OKAMURA and T. HIGAI, “PROPOSED DESIGN EQUATION FOR SHEAR STRENGTH OF REINFORCED CONCRETE BEAMS WITHOUT WEB REINFORCEMENT,” *Proc. Japan Soc. Civ. Eng.*, vol. 1980, no. 300, 1980, doi: 10.2208/jscej1969.1980.300_131.

[25] C. Andrade, C. Alonso, and F. J. Molina, “Cover cracking as a function of bar corrosion: Part I-Experimental test,” *Mater. Struct.*, vol. 26, no. 8, pp. 453–464, 1993, doi: 10.1007/BF02472805.

[26] B. Šavija, M. Luković, J. Pacheco, and E. Schlangen, “Cracking of the concrete cover due to reinforcement corrosion: A two-dimensional lattice model study,” *Constr. Build. Mater.*, vol. 44, 2013, doi: 10.1016/j.conbuildmat.2013.03.063.

[27] J. Baker, B. Bradley, and P. Stafford, *Seismic hazard and risk analysis*. Cambridge University Press, 2021.

[28] K. Porter, “A Beginner’s Guide to Fragility, Vulnerability, and Risk,” in *Encyclopedia of Earthquake Engineering*, 2021.

[29] K. Pitilakis, H. Crowley, and A. M. Kaynia, “SYNER-G: Typology Definition and Fragility Functions for Physical Elements at Seismic Risk: Buildings, Lifelines, Transportation Networks and Critical Facilities,” *Geotech. Geol. Earthq. Eng.*, vol. 27, 2014, doi: 10.1007/978-94-007-7872-6.

[30] R. O. Hamburger, “FEMA P58 seismic performance assessment of buildings,” 2014, doi: 10.4231/D3ZW18S8N.

[31] F. Cui, H. Zhang, M. Ghosn, and Y. Xu, “Seismic fragility analysis of deteriorating RC bridge substructures subject to marine chloride-induced corrosion,” *Eng. Struct.*, vol. 155, 2018, doi: 10.1016/j.engstruct.2017.10.067.